# Preparation of oriented cadmium sulfide nanocrystals

**Z. Y. Pan, G. J. Shen, L. G. Zhang, Z. H. Lu and J. Z. Liu**

*National Laboratory of Molecular and Biomolecular Electronics, Southeast University, Nanjing, 210096, China*

Cadmium sulfide (CdS) particulate films, composed of highly oriented, rod-like nanocrystals have been generated *in situ* by the exposure of stearic acid (SA) Langmuir monolayer-coated aqueous $CdCl_2$ solutions to hydrogen sulfide ($H_2S$). The SA-coated CdS particulate films were transferred to a solid substrate and examined by transmission electron microscopy (TEM) and Auger electron energy spectroscopy. It was found for the first time that the electron diffraction pattern was a composite one with six sets of diffraction patterns which were contributed by the different oriented CdS nanocrystals in these particulate films system. The epitaxial growth of rod-like CdS nanocrystals has been rationalized in terms of matching the $d_{220}$ spacing of the cubic CdS crystals and the $d_{10\bar{1}0}$ spacing of the hexagonal closed-packed SA monolayer. The presence of a negatively charged monolayer at the air/water interface was an essential requirement for the oriented growth of CdS nanocrystals. This leads to a novel means of fabrication of highly oriented semiconductor quantum wires.

Quantum confinement effects in semiconductor systems with reduced space dimensions have attracted considerable attention.[1–9] In this field, it is very important to assemble semiconductor nanocrystals in an orderly form and, at the same time, maintain the properties of each individual nanoparticle.[9–13]

Fendler's group first recognized that semiconductor nanoparticles can be synthesized by exposing fatty acid monolayer-coated aqueous salt solutions to small molecule gases.[14] The preparation of PbS and PbSe particulate films composed of high-oriented equilateral-triangular nanocrystals and some other particulate films have been reported in detail.[14–21] Because of the advantages of versatility and simplicity, Fendler's method is a very interesting, significant and attractive one for the formation of inorganic semiconductor nanocrystals in an orderly form. The Langmuir monolayer at the air/water interface not only provides size, geometrical control and stabilization with a single dimension for nanocrystals, but also influences the structure of the particulate films.[22–24] After the successful preparation of CdS monolayers within LB films and copper layers at the monolayer/subphase interface,[24–26] we have tried to prepare oriented CdS particulate films induced by an organic monolayer at the air/water interface.

TEM analyses of these semiconductor particulate films have been published and growth models proposed, but not enough attention has been paid to some interesting and detailed phenomena in these semiconductor systems (for example, the composition of the oriented CdS nanocrystals films). Recently, we reported that cadmium sulfide particulate films composed of highly oriented rod-like CdS nanocrystals can be prepared at the monolayer/subphase interface by exposing the stearic acid Langmuir monolayer-coated salt solution to hydrogen sulfide gas. The generation of CdS was proved by the Auger electron spectrum. Dark field images in TEM and transmission electronic diffraction were used to investigate the structure of the CdS particulate film in detail. It was found for the first time that the electron diffraction pattern was a composite one with six sets of individual electron diffraction patterns which implied that the CdS particulate films are composed of six sets of CdS nanocrystals. From the consideration of the electron diffraction pattern, a growth mechanism for the CdS particulate films was proposed and, at the same time, the epitaxial growth of the rod-like CdS nanocrystals was reasonably attributed to the matching of the distance of the (220) plane of the CdS crystals and the $\{10\bar{1}0\}$ planes of the hexagonal closed-packed SA monolayer.

## Experimental

The materials and the assembly method are similar to those reported earlier.[14–21]

The solution (in chloroform, $1 \times 10^{-3}$ mol dm$^{-3}$) of SA was spread on a four-times distilled water subphase containing $CdCl_2$ at a concentration of *ca.* $2 \times 10^{-4}$ mol dm$^{-3}$ and $NaHCO_3$ at a concentration of *ca.* $3 \times 10^{-4}$ mol dm$^{-3}$ at

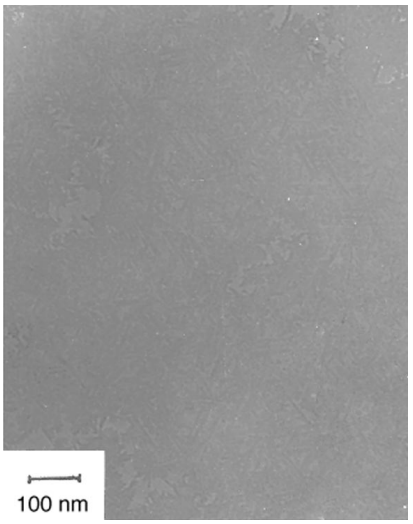


**Fig. 1** Typical TEM image of the CdS particulate films

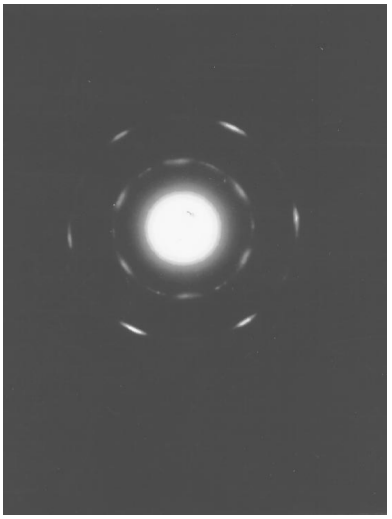

**Fig. 2** Electron diffraction pattern of the CdS particulate film in Fig. 1

pH = 6.42. The *in situ* generation of monolayer-supported CdS semiconductor particulate films was achieved as follows. In a rectangular trough the surface of the subphase was cleaned by sweeping it with an aspirator. The SA Langmuir monolayer were compressed to their solid states to give a coverage of 20 $Å^2$ molecule$^{-1}$. Injection of $H_2S$ at 100 μl $h^{-1}$ to the air/water interface led to the slow growth of CdS particulate films at the monolayer/subphase interface.

These CdS particulate films were prepared through the reaction of $H_2S$ and $Cd^{2+}$ at the monolayer/subphase interface. The presence of the SA monolayer plays an important role in the formation of the CdS particulate films. In order to avoid changing the deposition procedure,[27] the horizontal transferring method was chosen to transfer the monolayer-supported CdS particulate films to the substrate after the reaction.

After 2 h reaction, the monolayer-supported CdS particulate films were transferred to solid substrates by horizontal lifting through the surface layers. Amorphous carbon and formvar-coated 300 mesh copper grids and fresh, well cleaned silica were used as the substrates for transmission electron microscopy and Auger electron spectroscopy, respectively. TEM observations were carried out by a JEOL-2000EX electron microscope operating at 160 kV. Electron diffraction patterns of individual crystallites were also taken in the selected area. Auger electron spectroscopy was performed in a AES-350 Auger electron spectrometer.

## Results and Discussion

The present system is different from bulk semiconductors and from dispersed semiconductor particles. It is a highly oriented particulate film which consists of a large number of uniform

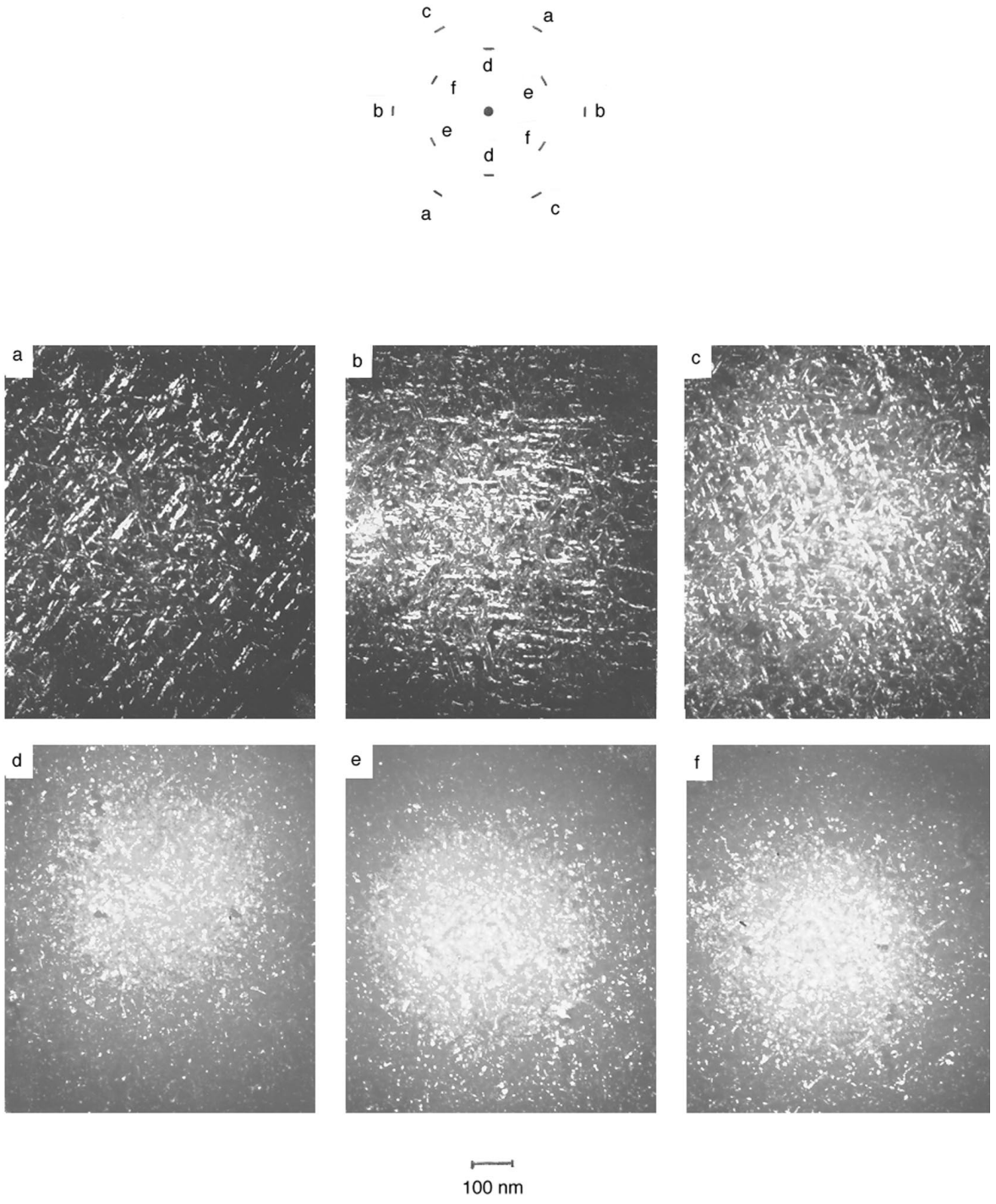


**Fig. 3** Top: The composite diffraction pattern composed of six sets of diffraction spots. Spots a–f were contributed by the crystals shown in a–f.

rod-like CdS nanocrystals. TEM is a very powerful tool because it allows us to see the arrangements, sizes and other important physical characteristics of the crystallites.[28] The combination of the TEM dark field image with an electron diffraction pattern enables us to investigate the structure and the growth mechanisms of these particulate films.

Fig. 1 is a typical TEM image of a CdS particulate film. The rod-like CdS particles of length *ca.* 100 nm aligned in three directions. These three directions were parallel to the edge directions of an equilateral triangle. Some dot-like CdS particles with no regular shape were found also. Because the film is very thin, the bright light image is not very clear. Longer reaction times could result in thicker films which are more readily observed, leading to the formation of the layer-by-layer structure, such a multilayer structure would be very difficult to analyse.[14–21] Fortunately, the combination of the electron diffraction pattern and the corresponding TEM dark field image enables us to see the morphology and composition of the particulate films clearly.

Fig. 2 is the transmission electron diffraction pattern from the area shown in Fig. 1, displaying a symmetric pattern with somewhat dispersed and elongated spots. This implies that the CdS nanocrystals are not oriented randomly. The orientation within the distribution is limited, *i.e.* there is pronounced texture. The TEM pattern shows that the diffraction arches should be indexed as the (220) (outer circle) and (111) (inner circle) faces of the CdS cubic lattice of the zinc-blende structure.[29] In order to analyse the composition and the growth mechanisms of CdS microcrystals under the SA Langmuir monolayer, the TEM dark field image technique was used. The results were totally different from those found for PbSe particulate films. It was found that the adjacent arches in one diffraction circle and the arches in the different diffraction circles were contributed by different CdS nanocrystals. Only the two arches symmetrical about the diffraction centre (symmetric inversion) were contributed by the same CdS nanocrystals, as shown in Fig. 3 (top). These two symmetrical arches compose a set of diffraction patterns. Six sets of individual electron diffraction patterns compose the diffraction pattern of CdS particulate films *i.e.* the diffraction pattern is actually a composite one. The different dark field images, corresponding to different sets of diffraction arches are shown in Fig. 3(a)–(f) respectively. In Fig. 3(a)–(c) the CdS nanocrystals were aligned in only one direction, but these three directions were different. The nanocrystallites in Fig. 3(d)–(f) were dot-like. In this experiment, the magnetic rotation angle of the TEM was 186°, the long axes of the rod-like CdS crystals in Fig. 3(a)–(c) were parallel to the line connecting the two corresponding diffraction arches and, at the same time, these three directions were parallel to the edges of an equilateral triangle as shown in Fig. 1 and Fig. 3.

It was mentioned above that the CdS crystallites were formed by the exposure of the SA monolayer-coated $CdCl_2$ solution to $H_2S$ gas. The surface charge density due to the head groups of the monolayer are important. Because of ionization of the carboxyl head groups of SA, negatively charged SA monolayers in their solid state consist of $CH_3(CH_2)_{16}COO^-$ ions which are ordered two-dimensionally at the air/water interface. The electrostatic attraction between the positively charged $Cd^{2+}$ and the negatively charged head group of the monolayer will lead to a very high $Cd^{2+}$ concentration at the monolayer/subphase interface where the nucleation of CdS nanocrystals is initiated. The preferential two-dimensional growth of the CdS crystallites is also reasonably attributed to the high local reagent concentration at the monolayer/subphase interface. Therefore the structure of the head group (monolayer) plays an important role in the fabrication of the CdS particulate films.

If the SA monolayer is compressed to its solid state, the carboxylate groups are aligned perpendicular to the water surface. The alkyl chains of SA, fully extended in the air in a planar zigzag conformation, are oriented approximately normal to the surface in a hexagonal close-packed lattice.[14–21] The hexagonal close-packed structure of the monolayer at the air/water interface has been discussed previously.[27,30,31] Fig. 4 shows the proposed hexagonal close-packed structure of the monolayer. From the structure of the monolayer and the area per molecule (20 $Å^2$), it is shown easily that the lattice constant $a$ is 4.81 Å.

The diffraction pattern of Fig. 2 shows that the $d_{220}$ and $d_{111}$ spacings of cubic CdS crystal are 1.94 Å and 3.16 Å respectively. A comparison of the double $d_{220}$ spacing of the CdS crystallites with $d_{10\bar{1}0}$ of the SA monolayer (4.16 Å) revealed a 6.8% mismatch between the template and the crystals. The morphology of these rod-like CdS nanocrystals [Fig. 1, 3(a)–(c)] is rationalized by the small mismatch (good fit) between $d_{220}$ of the CdS crystals and $d_{10\bar{1}0}$ of the hexagonal close-packed SA monolayer. This is illustrated in detail in Fig. 5. Thus the preferred orientation of the [110] axis of the CdS crystal is parallel to the monolayer and perpendicular to the electron beam. Therefore the rod-like CdS crystallites parallel to the edge directions of an equilateral triangle are reasonably attributed to the three equivalent $(10\bar{1}0)$ planes of the hexagonal close-packed SA monolayer.

There is a 30° angle between the line connecting the two diffraction arches produced by the corresponding rod-like CdS nanocrystals and that of the adjacent diffraction arches produced by the corresponding dot-like CdS nanocrystals. This result implies that the dot-like CdS nanocrystals were induced by the $\{11\bar{2}0\}$ planes of the hexagonal close-packed SA monolayer because the same angle is found between the $[10\bar{1}0]$ and $[11\bar{2}0]$ axes of the SA monolayer. The mismatch between the $d_{111}$ spacing (3.16 Å) of the CdS crystal and the $d_{11\bar{2}0}$ spacing (4.81 Å) of the SA monolayer is 31.7%. On the other hand, the mismatch between the double $d_{111}$ spacing of the CdS crystal and the $d_{11\bar{2}0}$ spacing of the SA monolayer is 34.2%.

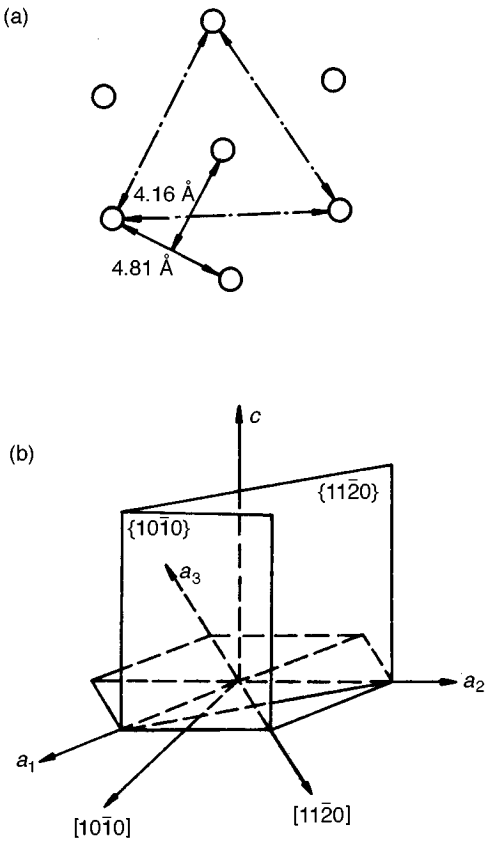


**Fig. 4** The hexagonal close-packed structure of the SA monolayer: (a) plan view; (b) three-dimensional representation

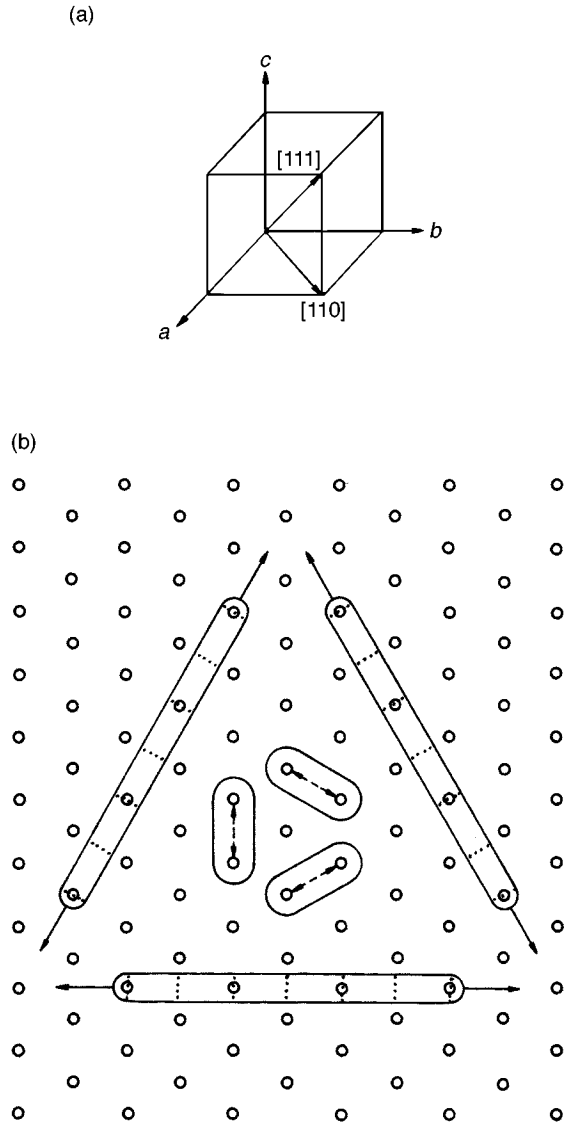


**Fig. 5** (a) The crystal structure of the cubic CdS crystal and (b) schematic diagram of the different CdS nanocrystal growth orientations. ——>, Growth direction of the rod-like crystals; ------>, growth direction of the dot-like crystals.

In other words, the mismatch between these two kinds of crystals faces is difficult to accommodate. The greater mismatch compared with that of the $d_{220}$ spacing of the CdS crystal and the SA monolayer (6.8%) resulted in the morphology of the dot-like nanocrystals [Fig. 3(d)–(f)]. Although the preferred growth orientation of dot-like CdS crystallites is [111] and this direction is perpendicular to the electron beam, the crystallites cannot grow long enough to produce rod-like morphology. This result is shown in Fig. 5, which shows the hexagonal close-packed structure of the Langmuir monolayer.

The generation of CdS was also studied by surface Auger electron spectroscopy (Fig. 6). Auger electron spectroscopy shows that the Cd : S ratio was *ca.* 1 : 1.[32]

The PbSe studied in earlier work had a face-centred cubic structure,[29] similar to CdS. It was found that the morphologies of the PbSe particulate films were different at different surface pressures, in other words the surface pressure of the Langmuir monolayer influences the morphology of the particulate film. We found that the pH of the subphase was another important factor which influences the morphology of the particulate film. In our experiment, $NaHCO_3$ was used to adjust the pH of the subphase. We will report the influence of the subphase pH and the surface pressure on the morphology of the CdS particulate

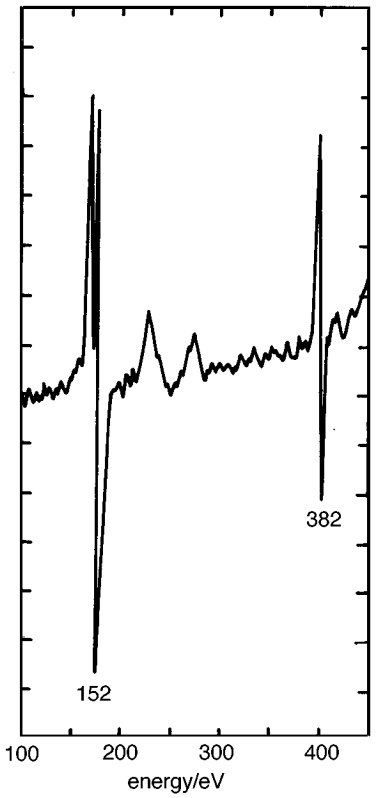


**Fig. 6** Auger electron spectrum of the surface of the CdS particulate films. $Cd:S=(H_{Cd}/0.98):(H_S/0.67)\approx 1$ (0.98 and 0.67 are the sensitivity factors of Cd and S respectively[29]).

films formed at the monolayer/liquid interface in a future paper.

The sizes (width 5–10 nm, length 100 nm) of each individual rod-like CdS crystallite are size-quantized; their sizes are comparable to the de Broglie electron wavelength, the mean free paths of excitons.[21–26,33] This implies that the rod-like CdS is a kind of quantum wire, which may lead to novel applications and devices.

The reaction of a monolayer-covered subphase with small gaseous molecules provides a potential method for nanofabrication of quantum dots and quantum wires. The most important factor in the preparation of this quantum confinement system is the match of the crystal and the template (the monolayer on the surface of the subphase), in other words the match of the face distances of the two kinds of crystal structures. If the semiconductor and the monolayer are suitable, the fabrication of perfect and highly oriented quantum wires is possible. This result opens the door to the colloid chemical generation of semiconductors with unusual crystal structures and controllable dimensions with unique electric, optical and electro-optical properties.

The other important phenomenon is that diffraction spots were observed instead of the usual diffraction arches. This was due to the structure of the compressed monolayer, which was not a strict hexagonal close-packed structure. It was also the reason why the rod-like CdS particles were not strictly aligned in one direction; there were small direction differences for different CdS rod-like crystallites. This implies that the structure of the monolayer is the other important and necessary factor for the fabrication of highly oriented quasi-two-dimensional quantum wire structures.

The authors thank the reviewers for very informative suggestions.

## References


1 L. E. Brus, *IEEE J. Quantum Electron*., 1986, **22**, 1909.
2 R. R. Chandler and J. L. Coffer, *J. Phys. Chem*., 1993, **97**, 9767.
3 H. Weller, *Angew. Chem., Int. Ed. Engl*., 1993, **32**, 41.
4 A. Mews, A. Eychmuller, M. Giersig, D. Schooss and H. Weller, *J. Phys. Chem*., 1994, **98**, 934.
5 Y. Wang and N. Herron, *J. Phys. Chem*., 1991, **95**, 525.
6 H. Weller, *Adv. Mater*., 1993, **5**, 88.
7 Y. Wang and N. Herron, *Phys. Rev. B*, 1992, **42**, 42.
8 L. Blus, *Appl. Phys. A*, 1991, **53**, 465.
9 V. L. Clvin, A. N. Goldstein and A. P. Alivisatos, *J. Am. Chem. Soc*., 1992, **114**, 5221.
10 J. R. Heath, *Science*, 1995, **270**, 1315; C. B. Murray, C. R. Kagan and M. G. Bawendi, *Science*, 1995, **270**, 1335.
11 C. R. Martin, *Science*, 1994, **266**, 1961.
12 S. Mann, *Nature* (*London*), 1993, **365**, 499.
13 I. Meriguchi, I. Tanaka, Y. Teraoka and S. Kagawa, *J. Chem. Soc., Chem. Commun*., 1991, 1401.
14 X. K. Zhao, Y. Yuan and J. H. Fendler, *J. Chem. Soc., Chem. Commun*., 1990, 1248.
15 X. K. Zhao, L. D. McCormick and J. H. Fendler, *Chem. Mater*., 1991, **3**, 922.
16 X. K. Zhao and J. H. Fendler, *Chem. Mater*., 1991, **3**, 168.
17 X. K. Zhao, S. Q. Xu and J. H. Fendler, *Langmuir*, 1991, **7**, 520.
18 X. K. Zhao, L. D. McCormick and J. H. Fendler, *Langmuir*, 1991, **7**, 1255.
19 X. K. Zhao and J. H. Fendler, *J. Phys. Chem*., 1991, **95**, 3716.
20 X. K. Zhao and J. H. Fendler, *J. Phys. Chem*., 1992, **96**, 9933.
21 J. Yang, J. H. Fendler, T. C. Jao and T. Laurion, *Microsc. Res. Tech*., 1994, **27**, 402.
22 B. R. Heywood, S. Rajam and S. Mann, *J. Chem. Soc., Faraday Trans*., 1991, **87**, 727; 735.
23 B. R. Heywood and S. Mann, *J. Am. Chem. Soc*., 1992, **114**, 4681.
24 G. P. Luo, Z. M. Ai, J. J. Hawkes, Z. H. Lu and Y. Wei, *Phys. Rev. B*, 1993, **48**, 15337 and refs. therein.
25 Z. Y. Pan, X. G. Peng, Z. H. Wu, T. J. Li, M. Zhu and J. Z. Liu, *Langmuir*, 1996, **12**, 851.
26 Z. Y. Pan, X. G. Peng, T. J. Li and J. Z. Liu, *Chin. J. Sci. Instrum*., 1996, **17**, 153.
27 V. K. Gupta, J. A. Kornfield, A. Ferencz and G. Wegner, *Science*, 1994, **265**, 940.
28 A. P. Alivisatos, *MRS Bull*., 1995, **XX**, 23.
29 O. Osugi *et al*., *Rev. Phys. Chem. Jpn*., 1966, **36**, 59; Joint Committee on Power Diffraction Stands, 1971.
30 J. B. Peng and G. T. Barnus, *Thin Solid Films*, 1994, **252**, 44.
31 R. Viswanathan, L. L. Madsen, J. A. Zasadzinski and D. K. Schwartz, *Science*, 1995, **269**, 51.
32 *Auger Electron Spectra Catalogue, A Data Collection of Elements*, Anelva Corporation, 1979.
33 Y. Wang, *Acc. Chem. Res*., 1991, **24**, 133.


*Paper* 6/04867F; *Received* 10*th July*, 1996